*Journal of Power Sources*, 46 (1993) 203–210 

# Location of the phenomena of premature capacity loss during cycling of lead/acid batteries with lead grids

M.K. Dimitrov and D. Pavlov
*Central Laboratory of Electrochemical Power Sources, Bulgarian Academy of Sciences, Sofia 1113 (Bulgaria)*

**Abstract**

Investigations of lead/acid cells with specially designed positive plates containing pure-lead and lead–antimony subgrids under various cycling modes have been performed. It has been established that the phenomena causing premature capacity loss proceed both in the corrosion layer and at its interfaces with the grid metal and the active material. Additions of antimony to the positive active mass do not improve substantially the life of cells prepared with positive plates based on pure-lead grids.

## Introduction

The performance of lead/acid batteries operated under deep-discharge conditions is usually determined by the properties of the positive plate. In the case of positive plates based on antimony alloy grids, the capacity decline with battery service is associated with progressive structural degradation of the positive active material (PAM). This is manifested by softening and shedding, and/or corrosion of the grid [1].

Positive plates based on antimony-free alloy grids exhibit a severe capacity loss in the first dozen or so cycles, on deep-discharge cycling, without any visible deterioration of the PAM. This phenomenon is commonly termed the 'antimony-free effect' (AFE) [2]. Recently, however, a similar behaviour of early capacity decline has been observed even in antimony-based systems under certain circumstances [3, 4]. Thus, the effect is better expressed as 'premature capacity loss' (PCL).

The explanations given for PCL can be divided into two groups:

(i) *Barrier corrosion layer models*. Insulating compounds are formed during discharge around the grid and prevent further discharge of the PAM. This assumes that the PAM can still deliver capacity and that the insulating compounds are an intrinsic property of the corrosion layer [5, 6].

(ii) *Active-material degradation models*. These describe a similar failure mode to that exhibited by antimonial plates, but at a higher rate for pure-lead plates [7], e.g., destruction of the agglomerate structure and crystallite size increase during cycling. Antimony modifies significantly the crystallinity, size, shape and connectivity of $PbO_2$ particles. Recently, a model of the PAM has been elaborated [8] based on the fact that the capacity loss can be restored. The increased resistance of the PAM, governed mainly by the resistance of interparticle contact zones, leads to a restricted material utilization and a consequent spread of the discharging reaction towards the corrosion layer.

The aim of the present paper is, first, to locate the sites in the structure of the positive plate where the phenomena causing premature capacity loss occur, second,

to demonstrate the effect of antimony on the current-generation processes that take place in both the active mass and the corrosion layer.

## Experimental

*Investigation methods and model cells*

All investigations were performed with model cells that comprised one positive and two negative plates assembled in cases with an excess of $H_2SO_4$ (sp. gr. 1.28). The plates were insulated by separators and the potential of the positive plate was determined versus a $Hg/Hg_2SO_4$ electrode. The effect of antimony on the behaviour of the corrosion layer was followed using a specially designed positive plate with two subgrids, one made of pure-lead (Pb) and the other one of lead–antimony alloy (Pb–Sb). The influence of antimony ions on the positive active mass was determined by applying the method described below.

The potential changes of the positive plates with lead and lead–antimony subgrids during discharge and on cycling of the cells were determined. Discharge was performed to 100% depth-of-discharge (DOD) at 47% utilization of the PAM. A current $I = 0.2$ $C_5$ was applied at a 5-h rate of discharge. One cycle was conducted each 24 h. This was a rather heavy mode of cycling, but it was deliberately chosen in order to allow the effect of antimony on the parameters of the positive plate to be manifested faster and more clearly.

The test electrodes were made with pure-lead and lead–antimony (Pb–4.5%wt.Sb) grids of size: 50 mm × 90 mm × 1.9 mm. The grids were pasted with a $3PbO \cdot PbSO_4 \cdot H_2O$ of density: 4.2 g $cm^{-3}$. Formation of the active mass was performed in $H_2SO_4$ (sp. gr. 1.05) with a current equal to 0.02 A per g of paste for 25 h. The formed positive plates were assembled into cells that were then subjected to investigation.

*Design of the plates with pure-lead and lead–antimony subgrids*

Up to now, the effect of antimony on the behaviour of the positive plate has been determined by comparing the results from cycling positive plates with Pb and Pb–Sb grids. In both cases, the active mass has been prepared by applying the same technology. Such an experimental setup, however, has limited capabilities. In the present investigation, a specially designed plate with two subgrids (Pb and Pb–Sb) stacked together with epoxy resin. The latter served also as an insulator between the two subgrids. The cell design in presented in Fig. 1(a). Each of the subgrids is a separate current collector through which cycling, charging and discharging of the plate was performed. The grids were pasted and the plates subjected to formation by applying the above-mentioned technology.

A schematic design of the cell containing one positive plate (with two subgrids) and two negative ones is presented in Fig. 1(b). PAM stands for the lead dioxide active mass. $Pb(CL_1)$ and $PbSb(CL_2)$ denote the lead and lead–antimony subgrids and the corrosion layers (CL) formed on them. RE refers to the $Hg/Hg_2SO_4$ reference electrode against which the plate potential was determined. $\varphi_1$ is the potential of the plate measured through the Pb subgrid, and $\varphi_2$ is the potential measured through the Pb–Sb subgrid. El stands for the electrolyte and the separators. NP marks the two negative plates and GS is the galvanostat. The cell can be connected to the galvanostat through the Pb subgrid (as shown in this Fig.) or through the Pb–Sb counterpart.

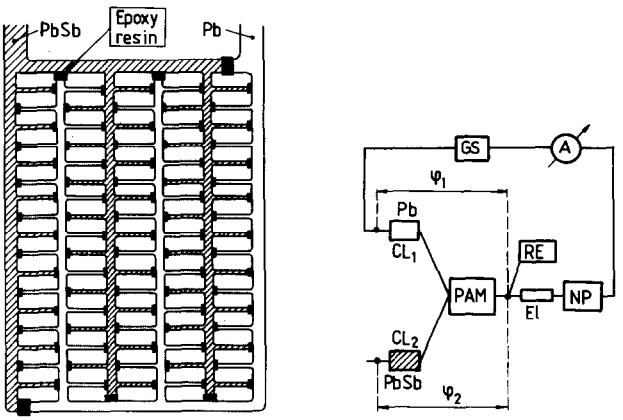


(a) (b)

Fig. 1. (a) Design of positive grid with Pb and Pb–Sb subgrids; (b) schematic design of the cell with a positive plate composed of Pb and Pb–Sb subgrids.

*Method for studying effect of antimony on PAM behaviour*

Antimony was introduced into the PAM both during formation and on cycling of the cells. Antimony ions were produced through anodic polarization of the Pb–Sb grid in the $H_2SO_4$ formation solution. Six such grids (3 positive and 3 negative) were cycled until the concentration of antimony ions in the solution reached 150 mg $l^{-1}$. Next, some of the grids were taken out of the solution and pasted plates were inserted for formation. The Pb–Sb grids were shorted to the positive plate so that the supply of antimony ions to the solution continued during formation. At the end of formation, the PAM contained about 0.05% antimony. This amount is close to the antimony content in the PAM of plates with Pb–4.5%wt.Sb grids.

To support the concentration of antimony in the solution during cycling, two Pb–6%wt.Sb grids under anodic polarization were used.

## Results

*Plate capacity during cycling cells through lead and lead–antimony subgrids*

Two identical cells containing one positive plate (with a Pb and a Pb–Sb subgrid) and two negative plates were investigated. One of the cells was connected through the current-collector of the Pb–Sb subgrid. The Pb current-collector was left at open circuit. The other cell was connected through the Pb current-collector (the Pb–Sb one was left at open circuit). Both cells were subjected to cycling at a 5-h rate of discharge, 100% DOD. Figure 2 presents the results obtained.

During the first 4 to 5 cycles, the capacities of the two cells are almost equal and reach 100% of the rated capacity. This indicates that each of the subgrids is sufficiently branched and capable of conducting the electric current to every point in the PAM. Each subgrid acts independently of the other one in the process of current generation.

When cycling is conducted through the Pb subgrid, the capacity of the cell declines to 1 Ah for 12 cycles. When cycled through the Pb–Sb subgrid, the cell exhibits a capacity very close in value to the rated one, even in the 32nd cycle. This indicates

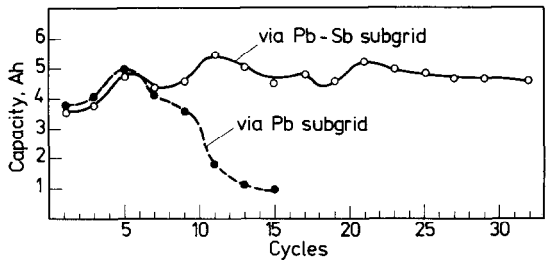


Fig. 2. Capacity changes on cycling the positive plate through the Pb or Pb–Sb subgrids.

that the plate capacity is determined not only by the processes occuring in the PAM, but also by the reactions that take place in the corrosion layer and at its interface with both the PAM and the metal of the two subgrids.

*Potential transients during discharge through lead and lead–antimony subgrids*

Two cells with positive plates with Pb and Pb–Sb subgrids were investigated. To allow the difference between the two subgrids to be clearly manifested, the cells were first subjected to 8 charge/discharge cycles. Then, the changes in plate potential versus the reference electrode were studied for the two types of subgrids (Fig. 1(b)). Figure 3 presents the changes in potential of the two subgrids during discharge of the cell through: curve (a) the Pb subgrid; curve (b) the Pb–Sb subgrid; curve (c) first through the Pb subgrid and then through the Pb–Sb one. The following conclusions can be drawn:

(i) When discharge is performed through the Pb subgrid, the composition of the corrosion layer and of its interfaces is changed. This leads to rapid polarization of the plate. The PAM is not fully discharged. The potential of the Pb–Sb subgrid is determined by the $PbO_2$ active mass and is approximately equal to 1.20 V.

(ii) When discharge of the plate is performed through the Pb–Sb subgrid, the potentials of the two subgrids have almost equal values throughout the whole discharge of the plate. In this case, the potentials of the two subgrids are determined by the processes occurring in the PAM during discharge.

(iii) Discharge of the positive active mass could proceed even if the plate is polarized through the Pb subgrid first and then the discharge is completed through the Pb–Sb subgrid. Antimony modifies the corrosion layer and its interfaces in such a way that the plate capacity is limited by the PAM, i.e., antimony blocks the capacity limiting effect of the processes occurring in the corrosion layer and its interfaces.

*Behaviour of cells on consecutive cycling through one of the two subgrids*

The behaviour of the cells was examined when cycled through the Pb subgrid first and, when the capacity had declined down to about 1 Ah (after about 12 cycles), cycling was completed through the Pb–Sb subgrid. Another test cell was cycled first through the Pb–Sb subgrid for 12 cycles (equal to the number of cycles needed for the capacity of the cell to decline when cycled through the Pb subgrid), and then cycling was continued through the Pb subgrid. The results obtained from these investigations are presented in Fig. 4.

The above electrode design allows the potentials to be applied to the corrosion layer of one of the subgrids through its metal grid or via the active material by polarization of the plate through the other subgrid. The results presented in Fig. 4(a)

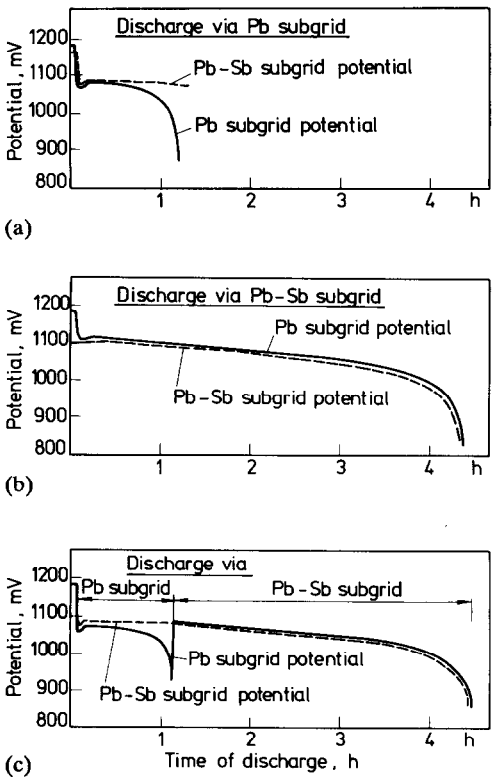


Fig. 3. Potential transients of positive plates on discharge: (a) through the Pb subgrid; (b) through the Pb–Sb subgrid; (c) first through the Pb subgrid, then through the Pb–Sb subgrid.

show that, irrespective of the site of potential input, the phase composition and the structure of the corrosion layers formed on each subgrid depend on the potential of the plate. Thus, although the Pb subgrid does not control the process of cycling (this is done by the Pb–Sb subgrid), a passivating corrosion layer is formed on the surface of the Pb subgrid and hence only part of the PAM capacity can be delivered through it (Fig. 4(b)). Second, both the structure and the phase composition of the corrosion layer are similar to those for the layer formed during plate polarization through the Pb subgrid.

On the other hand, these investigations confirm the conjecture that each subgrid can collect the current from the whole active mass independent of the other subgrid. The distance between the ribs of the subgrids is sufficient to prevent potentials drops in the PAM that would exclude part of the PAM from the process of current generation. (In the latter case, the capacity decline of the plate would depend on the design.)

Finally, in order to allow full realization of the capacity of the active mass, the phase composition, structure and electrical properties of the corrosion layer and of its interfaces should be such as to prevent a potential drop on current generation. When such potential barriers appears, the capacity is determined by both the corrosion layer and its interfaces. Utilization of the active material is restricted. The properties of the corrosion layer and of its interfaces depend strongly on the alloying additives

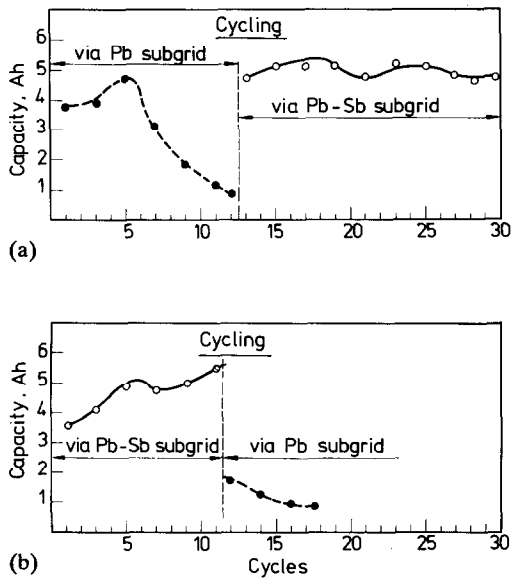


Fig. 4. Capacity changes on cycling: (a) first through the Pb subgrid, then through the Pb–Sb subgrid; (b) first through the Pb–Sb subgrid, then through the Pb subgrid.

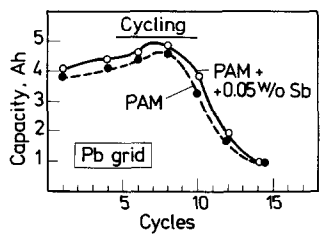


Fig. 5. Capacity changes on cycling of positive plates with Pb grids and PAM with/without antimony.

(in the case antimony). On grid corrosion, the alloying additives are also oxidized and become incorporated in the structure of the corrosion layer. This results in a modification of the electrical and mechanical performance of the layer.

*Effect of antimony on PAM properties*

Plates with Pb grids were used to study the effect of antimony on PAM behaviour. Antimony was introduced into the PAM through the solution used in plate-formation and in cycling (see above). The changes in capacity were studied during cycling of cells in $H_2SO_4$ and in antimony-rich $H_2SO_4$ solutions. The results are presented in Fig. 5 for one cell cycled in $H_2SO_4$ solution and another cell cycled in $H_2SO_4$ solution containing antimony ions.

Cells cycled in antimony-rich solutions have slightly higher capacity compared with those cycles in pure $H_2SO_4$ solutions. Both cells exhibit the same cycle life, and this corresponds to that of plates with Pb grids (Fig. 2).

## Discussion

The experimental results presented in Figs. 2 to 4 demonstrate clearly that, during cycling, the premature capacity decline in plates with pure-lead grids is due to phenomena that take place in the corrosion layer and at its interfaces. Within 8 to 10 cycles, a corrosion layer is formed on the surface of the lead grid which impairs the electrical performance of the plate. The latter is quickly passivated during discharge, whereby a considerable part of the PAM is excluded from the current generation process. The life of the battery is shortened.

When antimony is added to the lead grid the above phenomena that occur in the corrosion layer are blocked. Early polarization of the positive plate is prevented and the current-generation potential of the lead dioxide active mass is fully utilized. The role of antimony on restricting the phenomena leading to PCL effect has been discussed in ref. 9. It can be summarized as follows:

(i) Within a wide range of potentials, antimony maintains a high electric conductivity of the oxides formed in the corrosion layer. This is due to the electrocatalytic effect of antimony on the reaction of oxidation of the high-ohmic PbO in the corrosion layer to a low-ohmic, nonstoichiometric oxide, $PbO_n$ $(1.4 < n < 2)$ [10]. Thus, due to the beneficial effect of antimony the corrosion layer contains nonstoichiometric lead oxides ($PbO_n$ and $PbO_2$) and is highly conductive, over a wide potential range. In this way, the plate capacity is determined only by the properties of the PAM.

(ii) Antimony improves the elasticity of the corrosion layer and of its interfaces. This is a result of the high affinity of antimony for water. When its ions are incorporated into the structure of lead oxides, they increase the hydrated (gel) zones in the structure of the corrosion layer. These gel zones take over the mechanical stresses that occur as a result of the PAM volume pulsation on cycling and on oxidation of the lead grid [9]. Thus the risk of cracking of the corrosion layer and consequent mechanical deterioration of the PAM/grid contact is reduced [11].

The present investigations would hardly give evidence of the exact role of each of the above phenomena on the premature capacity loss of plates with pure-lead grids.

Figure 5 shows that when antimony is introduced into PAM through the working solution, it does not affect substantially the behaviour of the plates with Pb grids on cycling. Hence, the phenomena occurring in the PAM on cycling play only a minor role in the PCL effect. Under the applied experimental conditions used here, plates are cycled under a heavy regime. That is why the PCL effect is determined mainly by first-order phenomena (i.e., those with a most pronounced impact). It is quite possible that there are also phenomena in the PAM that contribute to the premature capacity loss of the plate, but these exert a second order of influence (i.e., only a weak effect). Figures 2 to 4 show that the first-order phenomena leading to PCL are located in the corrosion layer and at its interfaces.

## References

1 S.M. Caulder and A.C. Simon, *J. Electrochem. Soc., 121* (1974) 1546.
2 E.E. Schumacher and G.S. Phipps, *Trans. Electrochem. Soc., 68* (1935) 309.
3 W. Borger, U. Hullmeine, H. Laig-Horstebrock and E. Meissner, in T. Keily and B.W. Baxter (eds.), *Power Sources 12,* International Power Sources Symposium Committee, Leatherhead, Surrey, UK, 1989, p. 131.
4 A.F. Hollenkamp, K.K. Constanti, A.M. Huey, M.J. Koop and L. Apăteanu, *J. Power Sources, 40* (1992) 125.

5 K. Fuchida, K. Okada, S. Hattory, M. Kono, M. Yamane, T. Takayama, J. Yamashita and Y. Nakayama, *ILZRO Project LE-276, Final Rep., ILZRO,* 1982.
6 T.G. Chang, in K.R. Bullock and D. Pavlov (eds.), *Proc. Symp. Advances in Lead-Acid Batteries,* Vol. 84–14, The Electrochemical Society, Pennington, NJ, USA, 1984.
7 J. Burbank and E.J. Ritchie, *J. Electrochem. Soc., 117* (1970) 299.
8 A. Winsel, E. Voss and U. Hullmeine, *J. Power Sources, 30* (1990) 209.
9 D. Pavlov, *J. Power Sources, 46* (1993) 171–190.
10 B. Monahov, D. Pavlov, *Ext. Abstr., Proc. Int. Conf. on Lead/Acid Batteries: LABAT '93, St. Konstantin, Varne, Bulgaria, June 7–11, 1993,* p. 61.
11 D.A.J. Rand, *J. Power Sources, 23* (1988) 257.